Rotating Field Gradient (RFG) Diffusion MRI for Mapping 3D Orientation Distribution Functions (ODFs) in the Human Brain

Alexandru V Avram[1], Joelle E Sarlls[2], Peter J Basser[1], and Evren Ozarslan[3]

[1]*Section on Tissue Biophysics and Biomimetics, NICHD, National Institutes of Health, Bethesda, MD, United States,* [2]*NINDS, National Institutes of Health, Bethesda, MD, United States,* [3]*Department of Radiology, Brigham and Women's Hospital, Harvard Medical School, Boston, MA, United States*

Target Audience: Clinicians and basic scientists interested in mapping brain connectivity; pulse sequence programmers; MR scientists;

Introduction: Conventional methods for mapping 3D diffusion orientation distribution functions (dODFs) of neuronal microstructure such as QBI (1) or DSI (2) require the acquisition of a large number of DWIs, resulting in long scan durations and potential quantitation errors due to subject motion. In this study we describe a method for directly measuring *in vivo* 3D dODFs with a novel technique called Rotating Field Gradient (RFG) diffusion MRI (3). In RFG dMRI, sinusoidal diffusion gradient pulses are applied in a plane with arbitrary orientation yielding a rank-2 b-matrix (3, 4) and the sphere is sampled by varying the axis of rotation along different 3D orientations. The RFG diffusion signal is largest when the axis of rotation is along the direction of maximum diffusivity. Because this property holds for environments containing multiple slowly exchanging anisotropic Gaussian domains (such as brain tissue), the aggregate diffusion signal profile reflects the dODF directly, without the need for q-space analysis or analytical diffusion models.

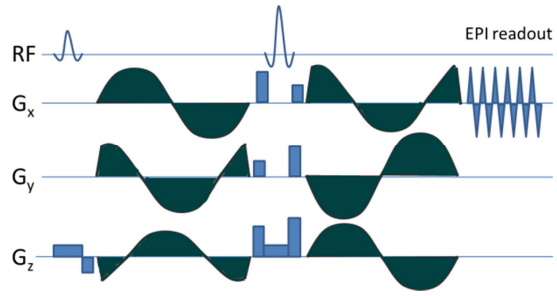

Fig. 1: Pulse sequence diagram for 3D RFG dMRI. Sinusoidal diffusion gradient waveforms are applied before and after the 180 RF pulse, with a 90° phase shift in the arbitrarily oriented plane of rotation.

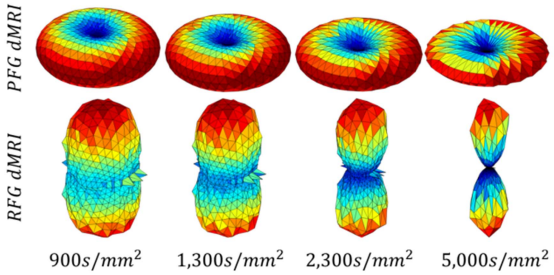

Fig. 2: Response functions for PFG (top row) and RFG (bottom row) diffusion preparations calculated for anisotropic Gaussian diffusion using different b-values.

Methods: A spin echo RFG DWI pulse sequence was implemented on a clinical scanner to allow the application of rotating diffusion gradients in a plane with arbitrary 3D orientation (Fig.1). To eliminate the signal dependence on the initial position within the plane of rotation, the second RFG waveform (i.e. the one following the 180° RF refocusing pulse) was applied with a 90° phase shift in the plane of rotation, yielding a rank-2 b-matrix necessary for planar diffusion weighting (3, 4). To visualize the response function of RFG dMRI we simulated the orientational dependence of the 3D RFG diffusion signal profile for anisotropic Gaussian diffusion (eigenvalues $\lambda_x=\lambda_y=0.6 mm^2ms^{-1}$, $\lambda_z=0.6$ mm^2ms^{-1}) and compared them with the corresponding profiles for PFG dMRI (Fig.2) for different b-values. Finally we evaluated the new technique *in vivo* by scanning a healthy volunteer using both the conventional PFG and the novel RFG single-shot diffusion EPI pulse sequences with the same imaging parameters: 25 slices with 5mm slice thickness, FOV=22x22cm², matrix size = 96x96, SENSE factor 2, and a TR=10s. The echo times were 83ms and 106ms for PFG and RFG dMRI, respectively.

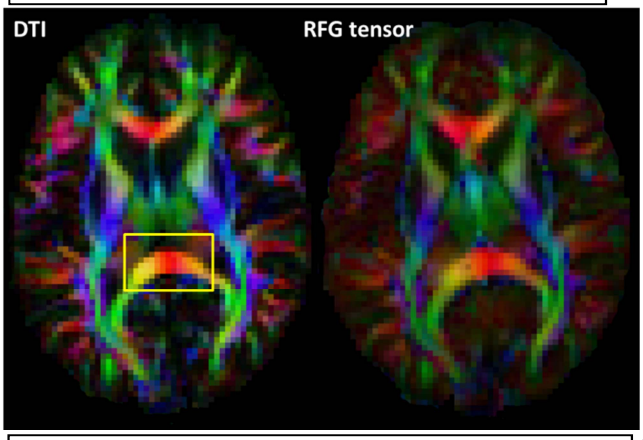

Fig. 4: The tensor model fitted directly to the RFG DWIs (right) reveals the same principal diffusion direction as the conventional PFG-derived DTI.

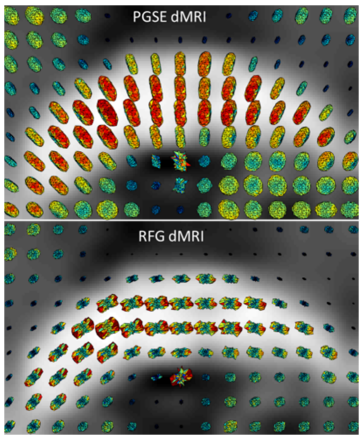

Fig. 3: *In vivo* PFG and RFG signal profiles in the splenium of the corpus callosum.

The PFG dMRI signal was sampled along 94 different orientations uniformly distributed along the unit sphere, while for RFG dMRI, rotating gradient pulses (40ms/cycle on each side of the 180 RF pulse) were applied in planes perpendicular to the same 94 directions with a b=1,200s/mm². All images were processed for motion and eddy current correction prior to analysis (5). Diffusion signal profiles for PFG and RFG dMRI were compared directly, and the orientation of white matter fibers was visualized by fitting a diffusion tensor model directly to the RFG DWIs and comparing the results to a conventional DTI reconstruction of the PFG DWIs (6).

Results and Discussion: The simulations confirm that the response function for RFG diffusion preparation directly follows the dODF, which is not the case in PFG dMRI (Fig. 2). Moreover, the RFG dMRI response function becomes sharper for larger b-values, suggesting a superior ability to resolve crossing fibers compared to PFG dMRI methods. As expected, *in vivo* maps indicate that the orientation of 3D RFG DWIs follow the local anatomy (Fig. 3) suggesting that this technique can be used to directly interrogate the dODF even in complex medial like neuronal tissue. This orientational dependence can be appreciated at a whole brain level in Fig. 4, which compares the direction encoded color (DEC) maps derived from PFG-based DTI and from the tensor model fit directly to the RFG DWIs and shows that they have the same preferred diffusion direction, despite the latter having lower values of fractional anisotropy. With the current scan parameters we observed no significant improvement in the ability of RFG dMRI to resolve crossing fibers compared to the PFG dMRI pulse sequence. However, as our numerical simulations predict, the fiber response function for RFG dMRI becomes significantly sharper at larger b-values potentially providing an alternative to PFG-based methods for resolving crossing fibers.

Conclusion: Our results demonstrate that using *in vivo* RFG dMRI, we can explicitly interrogate the dODF of brain tissue along arbitrary 3D orientations. Thus, RFG dMRI provides a simple, direct, and model-free method for mapping the dODFs with fewer acquisitions and quantitation errors due to the post-processing operations (e.g. q-space, or Funk-Radon Transform) required for PFG-based methods. With advances in gradient technology, larger b-values will enable sharper RFG dMRI response functions capable to separate crossing fibers with unmatched resolution.

References: 1. Tuch, MRM, 2004;52:1358-72; 2. Wedeen et al, MRM, 2005;54:1377-86; 3. Özarslan et al, ISMRM Scientific Workshop, 2013; 4. Westin et al, ISMRM Scientific Workshop, 2013; 5. Pierpaoli et al., ISMRM 2010;#1597; 6. Basser et al, Biophys J., 1994;66:259-267;